Inhibitory DNA Ligands to Platelet-Derived Growth Factor B-Chain

Louis S. Green,‡ Derek Jellinek,‡ Robert Jenison,‡ Arne Östman,§ Carl-Henrik Heldin,§ and Nebojsa Janjic*,‡

NeXstar Pharmaceuticals, 2860 Wilderness Place, Boulder, Colorado 80301, and Ludwig Institute for Cancer Research, Box 595, Biomedical Center, S-751 24 Uppsala, Sweden

Received June 26, 1996; Revised Manuscript Received August 20, 1996[⊗]

ABSTRACT: We have identified a group of DNA molecules that bind to platelet-derived growth factor (PDGF)-AB with subnanomolar affinity from a randomized DNA library using in vitro selection. Individual ligands cloned from the affinity-enriched pool bind to PDGF-AB and PDGF-BB with comparably high affinity ($K_d \approx 10^{-10}$ M) and to PDGF-AA with lower affinity ($>10^{-8}$ M), indicating specific recognition of the PDGF B-chain in the context of the hetero- or homodimer. The consensus secondary structure motif for most of the high-affinity ligands is a three-way helix junction with a three-nucleotide loop at the branch point. Photo-cross-linking experiments with 5-iodo-2′-deoxyuridine-substituted ligands establish a point contact between a thymidine nucleotide in the helix junction loop region and phenylalanine 84 of the PDGF-B chain. Representative minimal DNA ligands inhibit the binding of ^{125}I-PDGF-BB but not of ^{125}I-PDGF-AA to PDGF α- or β-receptors expressed in porcine aortic endothelial (PAE) cells in a concentration-dependent manner with half-maximal effects of ≈1 nM. The same ligands also exhibit a similar inhibitory effect on PDGF-BB-dependent [^{3}H]thymidine incorporation in PAE cells expressing the PDGF β-receptors. These DNA ligands represent a novel class of specific and potent antagonists of PDGF-BB and, by inference, PDGF-AB.

Platelet-derived growth factor (PDGF)[1] is a ubiquitous mitogen and chemotactic factor for many connective tissue cells that occurs as three disulfide-linked dimers composed of two homologous chains, A and B (Raines et al., 1990; Heldin, 1992). The biological function of PDGF is mediated through binding to two cell surface proteins, PDGF receptors α and β (Yarden et al., 1986; Matsui et al., 1988; Claesson-Welsh et al., 1989). Both receptor species contain five immunoglobulin-like extracellular domains, a transmembrane domain, and an intracellular tyrosine kinase domain. PDGF binding induces receptor dimerization which leads to autophosphorylation at specific intracellular tyrosine residues creating binding sites for several Src-homology 2 (SH2) domain-containing proteins and further transmission of chemotactic and mitogenic signals (Claesson-Welsh, 1994). Since the A-chain binds only to the α-receptor and the B-chain to both receptors with high affinity, the α-receptor homodimer binds all three PDGF isoforms, the αβ heterodimer binds PDGF-AB and PDGF-BB while the β-receptor homodimer binds only PDGF-BB with high affinity (Heldin et al., 1988, 1989; Seifert et al., 1989). Thus, the differences in cellular responses induced by the three PDGF dimers are governed by their receptor binding properties and the profile of receptor expression on target cells.

PDGF plays an important role in embryonic development. This is most clearly demonstrated in mice by targeted disruption of the PDGF B-chain gene (Levéen et al., 1994) or the PDGF β-receptor gene (Soriano, 1994). These mice die perinatally and exhibit a number of renal, cardiovascular, and hematologic abnormalities. Disruption of the PDGF A-chain gene also leads to lethality due to lung abnormalities (Boström et al., 1996). In the adult, in addition to being involved in wound healing processes, PDGF has been linked to the progression of a number of disease states (Raines et al., 1990; Heldin, 1992). In cancer, the loss of dependence on exogenous mitogenic stimulation for growth is one of the hallmarks of malignant transformation. Indeed, the first demonstration that growth factor expression was linked to malignant transformation came with the finding that the amino acid sequence of PDGF B-chain is virtually identical to that of p28sis, the transforming protein of simian sarcoma virus (SSV) (Doolittle et al., 1983; Waterfield et al., 1983). The ability of the PDGF-B gene and, to a lesser extent, the PDGF-A gene to transform cells that express the PDGF receptors is now well recognized (Beckmann et al., 1988; Bywater et al., 1988). Many tumor cell lines have since been shown to produce and secrete PDGF, some of which also express the cognate PDGF receptors; paracrine effect on the tumor stroma and, in some tumor cell lines, autocrine growth stimulation by PDGF are therefore possible (Raines et al., 1990; Heldin, 1992). In addition to cancer, PDGF has been implicated in other proliferative disease states. In atherosclerosis, PDGF contributes to arterial lesion formation mainly through its chemotactic effect on vascular smooth muscle cells (Lindner et al., 1995; Lindner & Reidy, 1995). In glomerulonephritis, the abnormal proliferation of mesangial cells appears to be driven by the PDGF-B/PDGF β-receptor autocrine loop (Iida et al., 1991).

In view of its importance in proliferative disease states, antagonists of PDGF may find useful clinical applications. Currently, antibodies to PDGF (Johnsson et al., 1985; LaRochelle et al., 1989; Vassbotn et al., 1990; Ferns et al., 1991; Herren et al., 1993) and the soluble PDGF receptors (Duan et al., 1991; Herren et al., 1993; Teisman & Hart,

* To whom correspondence should be addressed. Telephone: (303) 546-7637. Fax: (303) 444-5893. E-mail: janjic@nexstar.com.

‡ NeXstar Pharmaceuticals.

§ Ludwig Institute for Cancer Research.

⊗ Abstract published in *Advance ACS Abstracts,* November 1, 1996.

[1] Abbreviations: HSA, human serum albumin; IdU, 5-iodo-2′-deoxyuridine; PAE, porcine aortic endothelial; PBS, phosphate-buffered saline; PBSE, PBS with 1 mM EDTA; PBSM, PBS with 1 mM $MgCl_2$; PDGF, platelet-derived growth factor; SELEX, systematic evolution of ligands by exponential enrichment; SSV, simian sarcoma virus.

S0006-2960(96)01544-9 CCC: $12.00

1993) are the most potent and specific antagonists of PDGF. Neutralizing antibodies to PDGF have been shown to revert the SSV-transformed phenotype (Johnsson et al., 1985) and to inhibit the development of neointimal lesions following arterial injury (Ferns et al., 1991). Other inhibitors of PDGF such as suramin (Betsholtz et al., 1984; Williams et al., 1984), neomycin (Vassbotn et al., 1992), and peptides derived from the PDGF amino acid sequence (Engström et al., 1992) have been reported; however, they either are too toxic or lack sufficient specificity or potency to be good drug candidates. Another class of antagonists of possible clinical utility are tyrphostins which selectively inhibit the PDGF receptor tyrosine kinase (Kovalenko et al., 1994; Buchdunger et al., 1995).

Sequence-randomized nucleic acid libraries embody a vast multitude of binding specificities (Ellington & Szostak, 1990; Tuerk & Gold, 1990). Screening of these libraries with the SELEX (systematic evolution of ligands by exponential enrichment) combinatorial chemistry process has recently led to the discovery of high-affinity ligands to a large number of molecular targets (Eaton et al., 1995; Gold, 1995; Gold et al., 1995). We describe in this report the identification of DNA molecules selected from a random library for high-affinity binding to PDGF-AB. Most of the ligands from the final affinity-enriched pool share a common secondary structure motif novel to the SELEX-derived ligands: a three-way helix junction with a three-nucleotide loop at the branch point. These ligands bind to PDGF-AB and PDGF-BB with high affinity and to PDGF-AA with substantially lower affinity, indicating preferential recognition of the PDGF B-chain in the context of the hetero- or homodimer. Photo-cross-linking experiments with 5-iodo-2′-deoxyuridine-modified ligands establish a specific point contact between a nucleotide in the loop at the branch point and phenylalanine 84 of the PDGF B-chain. We show that representative minimal ligands inhibit binding of ^{125}I-PDGF-BB (but not of ^{125}I-PDGF-AA) to α- or β-receptors expressed in porcine aortic endothelial cells, as well as PDGF-BB-induced increase in DNA synthesis in porcine aortic endothelial cells transfected with the β-receptor.

MATERIALS AND METHODS

Materials. Recombinant human PDGF-AA (M_r = 29 000), PDGF-AB (M_r = 27 000), and PDGF-BB (M_r = 25 000) were purchased from R&D Systems (Minneapolis, MN) in lyophilized form, free from carrier protein. All three isoforms were produced in *Escherichia coli* from synthetic genes based on the sequences for the long form of the mature human PDGF A-chain (Betsholtz et al., 1986) and the naturally occurring mature form of human PDGF B-chain (Johnsson et al., 1984). Randomized DNA libraries, PCR primers, and DNA ligands and 5-iodo-2′-deoxyuridine-substituted DNA ligands were synthesized by NeXstar (Boulder, CO) or by Operon Technologies (Alameda, CA) using the standard solid phase phosphoramidite method (Sinha et al., 1984).

SELEX. The initial ssDNA library containing a contiguous randomized region of 40 nucleotides, flanked by primer annealing regions of invariant sequence (5′-CCGAAGCTTAATACGACTCACTATAGGGATCCGCCTGATTAGCGATACT-[40N]-ACTTGAGCAAAATCACCTGCAGGGG-3′), was synthesized by the solid phase phosphoramidite method. An equal molar mixture of the four phosphoramidites was used to generate the randomized positions. PCR primers used were 3N2 [5′-BBBCCCCTGCAGGTGATTTTGCTCAAGT-3′; where B designates biotin, from biotin phosphoramidite (Glen Research, Sterling, VA)] and 5N2 (5′-CCGAAGCTTAATACGACTCACTATAGGGATCCGCCTGATTAGCGATACT-3′; used in SELEX rounds 1−9) or truncated 5N2 (5′-ATCCGCCTGATTAGCGATACT-3′; used in SELEX rounds 10−12). The ssDNA library was purified by electrophoresis on an 8% polyacrylamide/7 M urea gel. The band that corresponds to the full-length DNA was visualized under UV light, excised from the gel, eluted by the crush and soak method, ethanol-precipitated, and pelleted by centrifugation. The pellet was dried under vacuum and resuspended in phosphate-buffered saline supplemented with 1 mM $MgCl_2$ (PBSM = 10.1 mM Na_2HPO_4, 1.8 mM KH_2PO_4, 137 mM NaCl and 2.7 mM KCl, 1 mM $MgCl_2$, pH 7.4) buffer. Prior to incubation with the protein, the ssDNA was heated at 90 °C for 2 min in PBSM and cooled on ice. The first selection was initiated by incubating approximately 500 pmol (3×10^{14} molecules) of 5′-^{32}P end-labeled random ssDNA with PDGF-AB in binding buffer [PBSM containing 0.01% human serum albumin (HSA)]. The mixture was incubated at 4 °C overnight, followed by a brief (15 min) incubation at 37 °C. The DNA bound to PDGF-AB was separated from unbound DNA by electrophoresis on an 8% polyacrylamide gel [1:30 bis(acrylamide):acrylamide] at 4 °C and at 5 V/cm with 89 mM Tris−borate (pH 8.3) containing 2 mM EDTA as the running buffer. The band that corresponds to the PDGF−ssDNA complex, which runs with about half the electrophoretic mobility of the free ssDNA, was visualized by autoradiography, excised from the gel, and eluted by the crush and soak method. In subsequent affinity selections, the ssDNA was incubated with PDGF-AB for 15 min at 37 °C in binding buffer, and the PDGF-bound ssDNA was separated from the unbound DNA by nitrocellulose filtration, as previously described (Green et al., 1995a). All affinity-selected ssDNA pools were amplified by PCR in which the DNA was subjected to 12−20 rounds of thermal cycling (30 s at 93 °C, 10 s at 52 °C, 60 s at 72 °C) in 10 mM Tris-HCl (pH 8.4) containing 50 mM KCl, 7.5 mM $MgCl_2$, 0.05 mg/mL bovine serum albumin, 1 mM deoxynucleoside triphosphates, 5 μM primers, and 0.1 unit/μL Taq polymerase. The 5′ PCR primers (5N2 or truncated 5N2) were 5′ end-labeled with polynucleotide kinase and [γ-^{32}P]ATP. Following PCR amplification, streptavidin (Pierce, Rockford, IL) was added to the unpurified PCR reaction mixture at a 10-fold molar excess over the biotinylated primer and incubated for 15 min at room temperature. The dsDNA was denatured by adding an equal volume of stop solution (90% formamide, 1% sodium dodecyl sulfate, and 0.025% bromophenol blue and xylene cyanol) and incubating for 20 min at room temperature. The radiolabeled strand was separated from the streptavidin-bound biotinylated strand by electrophoresis on 12% polyacrylamide/7 M urea gels (Pagratis, 1996). The faster migrating radiolabeled (nonbiotinylated) ssDNA strand was excised from the gel and recovered as described above. The amount of ssDNA was estimated from the absorbance at 260 nm using the extinction coefficient of 33 μg mL^{-1} (absorbance unit)$^{-1}$ (Sambrook et al., 1989).

Cloning and Sequencing. The amplified affinity-enriched pool was purified on a 12% polyacrylamide gel, cloned between *Hin*dIII and *Pst*I sites in the pUC18 vector, and introduced into the JM109 strain of *E. coli* by electroporation (Sambrook et al., 1989). Plasmid DNA from individual recombinant clones was isolated by alkaline lysis. The nucleotide sequence was determined by the dideoxynucleotide chain-termination method using Sequenase 2.0 (Amersham, Arlington Heights, IL) and the M13 primer according to the manufacturer's protocol.

Determination of the Apparent Equilibrium Dissociation Constants and the Dissociation Rate Constants. The binding of ssDNA ligands at low concentrations to varying concentrations of PDGF was determined by the nitrocellulose filter binding method as described (Green et al., 1995a). The concentrations of PDGF stock solutions (in PBS) were determined from the absorbance readings at 280 nm using the following ϵ_{280} values calculated from the amino acid sequences (Gill & von Hippel, 1989): 19 500 M^{-1} cm^{-1} for PDGF-AA, 15 700 M^{-1} cm^{-1} for PDGF-AB, and 11 800 M^{-1} cm^{-1} for PDGF-BB. ssDNAs for all binding experiments were purified by electrophoresis on 8% (>80 nucleotides) or 12% (<40 nucleotides) polyacrylamide/7 M urea gels. All ssDNA ligands were heated at 90 °C in binding buffer at high dilution (≈1 nM) for 2 min and cooled on ice prior to further dilution into the protein solution. The binding mixtures were typically incubated for 15 min at 37 °C before partitioning on nitrocellulose filters.

The binding of DNA ligands (L) to PDGF-AA (P) is adequately described with the bimolecular binding model for which the fraction of bound DNA at equilibrium (q) is given by eq 1:

$$q = (f/2[\mathrm{L}]_t)\{[\mathrm{P}]_t + [\mathrm{L}]_t + K_d - [([\mathrm{P}]_t + [\mathrm{L}]_t + K_d)^2 - 4[\mathrm{P}]_t[\mathrm{L}]_t]^{1/2}\} \quad (1)$$

where $[\mathrm{P}]_t$ and $[\mathrm{L}]_t$ are the total protein and total DNA concentrations, K_d is the equilibrium dissociation constant, and f is the efficiency of retention of protein−DNA complexes on nitrocellulose filters (Irvine et al., 1991; Jellinek et al., 1993).

The binding of DNA ligands to PDGF-AB and PDGF-BB is biphasic and can be described by a model in which the DNA ligand is composed of two noninterconverting components (L_1 and L_2) that bind to the protein with different affinities, described by corresponding dissociation constants, K_{d1} and K_{d2} (Jellinek et al., 1993). In this case, the explicit solution for the fraction of bound DNA (q) is given by eq 2:

$$q = f\left(\frac{\chi_1 K_{d1}}{1 + K_{d1}[\mathrm{P}]} + \frac{\chi_2 K_{d2}}{1 + K_{d2}[\mathrm{P}]}\right)[\mathrm{P}]$$

with

$$[\mathrm{P}] = \frac{[\mathrm{P}]_t}{1 + [\chi_1 K_{d1}[\mathrm{L}]_t/(1 + K_{d1}[\mathrm{P}])] + [\chi_2 K_{d2}[\mathrm{L}]_t/(1 + K_{d2}[\mathrm{P}])]} \quad (2)$$

where χ_1 and χ_2 ($=1 - \chi_1$) are the mole fractions of L_1 and L_2, respectively. The K_d values for the binding of DNA ligands to PDGF were calculated by fitting the data points to eq 1 (for PDGF-AA) or eq 2 (for PDGF-AB and PDGF-BB) using the Gauss−Newton nonlinear least-squares method (Bates & Watts, 1988).

The dissociation rate constants (k_{off}) were determined by measuring the amount of ^{32}P 5′-end-labeled minimal ligands (0.17 nM) bound to PDGF-AB (1 nM) as a function of time following the addition of a 500-fold excess of unlabeled ligands, using nitrocellulose filter binding as the partitioning method. The k_{off} values were determined by fitting the data points (Kaleidagraph, Reading, PA) to the first-order rate equation (eq 3):

$$(q - q_\infty)/(q_o - q_\infty) = \exp(-k_{off}t) \quad (3)$$

where q, q_o, and q_∞ represent the fractions of DNA bound to PDGF-AB at any time (t), $t = 0$, and $t = \infty$, respectively.

Minimal Ligand Determinations. To generate a population of 5′ end-labeled DNA ligands serially truncated from the 3′ end, truncated primer 5N2 was radiolabeled at the 5′ end with [γ-^{32}P]ATP and T4 polynucleotide kinase, annealed to the complementary strand of the ligand, and extended with Sequenase 2.0 (Amersham, Arlington Heights, IL) in a standard dideoxynucleotide chain-termination reaction. Following incubation in binding buffer for 15 min at 37 °C, the fragments from this population that retain high-affinity binding to PDGF-AB were separated from those with weaker affinity by nitrocellulose filter partitioning. Electrophoretic resolution of the fragments on 8% polyacrylamide/7 M urea gels, before and after affinity selection, allows determination of the 3′ boundary. To generate a population of 3′ end-labeled DNA ligands serially truncated from the 5′ end, the DNA ligands were radiolabeled at the 3′ end with cordycepin 5′-[α-^{32}P]triphosphate (New England Nuclear, Boston, MA) and T4 RNA ligase (Promega, Madison, WI), phosphorylated at the 5′ end with ATP and T4 polynucleotide kinase, and partially digested with lambda exonuclease (Gibco BRL, Gaithersburg, MD). Partial digestion of 10 pmol of 3′-labeled ligand was done in a 100 μL volume with 7 mM glycine−KOH (pH 9.4), 2.5 mM $MgCl_2$, 1 μg/mL bovine serum albumin, 15 μg of tRNA, and 4 units of lambda exonuclease for 15 min at 37 °C. The 5′ boundary was determined in an analogous manner to that described for the 3′ boundary.

Melting Temperature (T_m) Measurements. Melting profiles for the minimal DNA ligands were obtained on a Cary Model 1E spectrophotometer. Oligonucleotides (320−400 nM) were heated to 95 °C in PBSM or PBS with 1 mM EDTA (PBSE) and cooled to room temperature prior to the melting profile determination. Melting profiles were generated by heating the samples at the rate of 1 °C/min from 15 to 95 °C and recording the absorbance every 0.1 °C. The melting data were fitted with a two-state model (Petersheim & Turner, 1983) for ligands 20t and 41t or a three-state model (Dominic Zichi, unpublished results) for ligand 36t, using the Gauss−Newton nonlinear least-squares method (Bates & Watts, 1988).

Cross-Linking of 5-Iodo-2′-deoxyuridine-Substituted DNA Ligands to PDGF-AB. DNA ligands containing single or multiple substitutions of 5-iodo-2′-deoxyuridine for thymidine were synthesized using the solid phase phosphoramidite method. To test for the ability to cross-link, trace amounts of 5′-^{32}P end-labeled ligands were incubated with

PDGF-AB (100 nM) in binding buffer at 37 °C for 15 min prior to irradiation. The binding mixture was transferred to a 1 cm path length cuvette thermostated at 37 °C and irradiated at 308 nm for 25−400 s at 20 Hz using a XeCl-charged Lumonics Model EX748 excimer laser. The cuvette was positioned 24 cm beyond the focal point of a convergent lens, with the energy at the focal point measuring 175 mJ/pulse. Following irradiation, aliquots were mixed with an equal volume of formamide loading buffer containing 0.1% sodium dodecyl sulfate and incubated at 95 °C for 5 min prior to resolution of the cross-linked PDGF/ligand complex from the free ligand on 8% polyacrylamide/7 M urea gels.

To identify the protein site of cross-linking for ligand 20t-I4, binding and irradiation were done on a larger scale. PDGF-AB and 5′-^{32}P end-labeled ligand, each at 1 μM in PBSM, were incubated and irradiated (300 s) as described above in two 1 mL reaction vessels. The reaction mixtures were combined, ethanol-precipitated, and resuspended in 0.3 mL of Tris-HCl buffer (100 mM, pH 8.5). The PDGF-AB/ligand cross-linked complex was digested with 0.17 μg/μL modified trypsin (Boehringer Mannheim, Indianapolis, IN) for 20 h at 37 °C. The digest mixture was extracted with phenol/chloroform and chloroform and then ethanol-precipitated. The pellet was resuspended in water and an equal volume of formamide loading buffer with 5% (v/v) β-mercaptoethanol (without sodium dodecyl sulfate), incubated at 95 °C for 5 min, and resolved on a 40 cm 8% polyacrylamide/7 M urea gel. The cross-linked tryptic peptide/ligand that migrated as two closely spaced bands about 1.5 cm above the free ligand band was excised from the gel and eluted by the crush and soak method and ethanol-precipitated. The dried cross-linked peptide (about 160 pmol based on the specific activity) was sequenced by Edman degradation (Midwest Analytical, Inc., St. Louis, MO).

Receptor Binding Assay. The binding of ^{125}I-PDGF-AA and ^{125}I-PDGF-BB to porcine aortic endothelial (PAE) cells transfected with PDGF α- or β-receptors was performed as described (Heldin et al., 1988). Different concentrations of DNA ligands were added to the cell culture (1.5 cm^2) in 0.2 mL of phosphate-buffered saline supplemented with 1 mg of bovine serum albumin per milliliter together with ^{125}I-PDGF-AA (2 ng, 100 000 cpm) or ^{125}I-PDGF-BB (2 ng, 100 000 cpm). After incubation at 4 °C for 90 min, the cell cultures were washed- and cell-associated radioactivity was determined in a γ-counter (Heldin et al., 1988).

[^{3}H]Thymidine Incorporation Assay. The incorporation of [^{3}H]thymidine into PAE cells expressing PDGF β-receptor in response to 20 ng/mL PDGF-BB or 10% fetal calf serum and in the presence of different concentrations of DNA ligands was performed as described (Mori et al., 1991). After incubation for 24 h at 37 °C, ^{3}H-radioactivity incorporated into DNA was determined using a β-counter.

RESULTS

The SELEX Process. High-affinity DNA ligands to PDGF-AB were identified by the SELEX process from a library of ≈3 × 10^{14} molecules (500 pmol) of single-stranded DNA randomized at 40 contiguous positions. The PDGF-bound DNA was separated from unbound DNA by polyacrylamide gel electrophoresis in the first round and by nitrocellulose filter binding in the subsequent rounds. After 12 rounds of SELEX, the affinity-enriched pool bound to PDGF-AB with an apparent dissociation constant (K_d) of ≈50 pM (data not shown). This represented an improvement in affinity of ≈700-fold compared to the initial randomized DNA library. We used this affinity-enriched pool to generate a cloning library from which 39 isolates were sequenced. Thirty-two of these ligands were found to have unique sequences. To identify the best ligands from this group, we determined their relative affinities for PDGF-AB by measuring the fraction of 5′-^{32}P end-labeled ligands bound to PDGF-AB over a range of protein concentrations. For the ligands that bound to PDGF-AB with high affinity, the affinity toward PDGF-BB and PDGF-AA was also examined: in all cases, the affinity of ligands for PDGF-AB and PDGF-BB was comparable while the affinity for PDGF-AA was considerably lower (data not shown).

Table 1: Frequency of Base Pairs in the Helical Regions of the Consensus Motif Shown in Figure 2

	base pair[b]						
position[a]	AT	TA	GC	CG	TG	GT	other
I-1	0	0	21	0	0	0	0
I-2	0	0	21	0	0	0	0
I-3	5	0	16	0	0	0	0
I-4	3	5	1	4	1	0	7
II-1	0	1	2	17	0	0	1
II-2	5	5	5	1	0	4	1
II-3	3	4	7	6	0	0	1
II-4	3	0	8	5	0	0	4
III-1	21	0	0	0	0	0	0
III-2	0	10	0	11	0	0	0
III-3	0	7	0	13	1	0	0

[a] Helices are numbered with roman numerals as shown in Figures 1 and 2. Individual base pairs are numbered with arabic numerals starting with position 1 at the helix junction and increasing with increased distance from the junction. [b] We have included the TG and GT base pairs to the Watson−Crick base pairs for this analysis. There is a total of 21 sequences in the set.

Consensus Secondary Structure of High-Affinity DNA Ligands. Of the 32 unique ligands, 21 can be grouped into a sequence family shown in Figure 1. This classification is based in part on sequence homology among these ligands, but in greater part based on a shared secondary structure motif: a three-way helix junction with a three-nucleotide loop at the branch point (Figure 2). These ligands are subdivided into two groups; for ligands in group A, the loop at the branch point has an invariant sequence AGC, and in group B, that sequence is G(T/G)(C/T). The proposed consensus secondary structure motif is supported by base-pairing covariation at nonconserved nucleotides in the helices (Table 1). Since the three-way junctions are encoded in continuous DNA strands, two of the helices end in loops at the distal end from the junction. These loops are highly variable, both in length and in sequence. Furthermore, through circular permutation of the consensus motif, the loops occur in all three helices, although they are most frequent in helices II and III. Together these observations suggest that the regions distal from the helix junction are not important for high-affinity binding to PDGF-AB. The highly conserved nucleotides are indeed found near the helix junction (Figures 2, 3).

Minimal Sequence Determination. The minimal sequence necessary for high-affinity binding was determined for the six best ligands to PDGF-AB. In general, the information

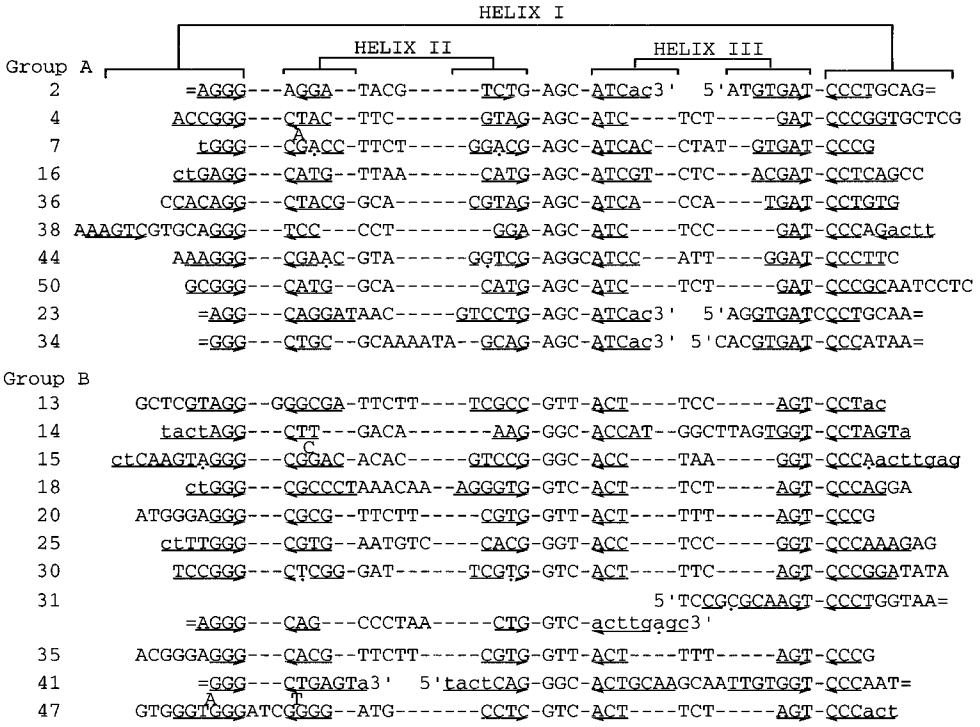

FIGURE 1: Evolved sequences of DNA ligands to PDGF-AB isolated from the final affinity-enriched pool. The sequences of the initially randomized region (uppercase letters) are aligned according to the consensus three-way helix junction motif. Nucleotides in the sequence-invariant region (lowercase letters) are only shown where they participate in the predicted secondary structure. Several ligands were "disconnected" (equality symbol) in order to show their relatedness to the consensus motif through circular permutation. The nucleotides predicted to participate in base pairing are indicated with underline-inverted arrows, with the arrowheads pointing toward the helix junction. The sequences are divided into two groups, A and B, based on the first single-stranded nucleotide (from the 5′ end) at the helix junction (A or G, between helices II and III). Mismatches in the helical regions are shown with dots under the corresponding letters (G-T and T-G base pairs were allowed). In places where single-nucleotide bulges occur, the mismatched nucleotide is shown above the rest of the sequence between its neighbors.

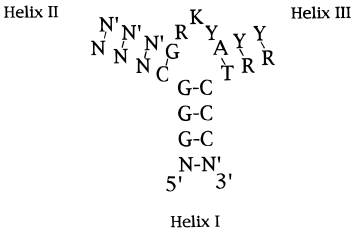

FIGURE 2: Consensus secondary structure for the sequence set shown in Figure 1. R = A or G, Y = C or T, K = G or T, and N and N′ indicate any base pair.

about the 3′ and 5′ minimal sequence boundaries can be obtained by partially fragmenting the nucleic acid ligand and then selecting for the fragments that retain high affinity for the target. With RNA ligands, the fragments can be conveniently generated by mild alkaline hydrolysis (Tuerk et al., 1990; Jellinek et al., 1994, 1995; Green et al., 1995a). Since DNA is more resistant to base, an alternative method of generating fragments is needed. To determine the 3′ boundary, a population of ligand fragments serially truncated at the 3′ end was generated by extending the 5′ end-labeled primer annealed to the 3′ invariant sequence of a DNA ligand using the dideoxy sequencing method. This population was affinity-selected by nitrocellulose filtration, and the shortest fragments (truncated from the 3′ end) that retain high-affinity binding for PDGF-AB were identified by polyacrylamide gel electrophoresis (Figure 3A). The 5′ boundary was determined in an analogous manner except that a population of 3′ end-labeled ligand fragments serially truncated at the 5′ end was generated by limited digestion with lambda exonuclease (Figure 3B). The minimal ligand is then defined as the sequence between the two boundaries. It is important to keep in mind that, while the information derived from these experiments is useful, the suggested boundaries are by no means absolute since the boundaries are examined one terminus at the time. The untruncated (radiolabeled) termini can augment, reduce, or have no effect on binding (Jellinek et al., 1994). Of the six minimal ligands for which the boundaries were determined experimentally, two (20t and 41t; truncated versions of ligands 20 and 41) bound with affinities comparable (within a factor of 2) to their full-length analogs, and four had considerably lower affinities. The two minimal ligands that retained high-affinity binding to PDGF, 20t and 41t, contain the predicted three-way helix junction secondary structure motif (Figure 4). The sequence of the third minimal ligand that binds to PDGF-AB with high affinity, 36t, was deduced from the knowledge of the consensus motif (Figure 4). To reduce 3′-exonuclease degradation, all minimal ligands were synthesized with a 3′-3′-linked thymidine nucleotide (Seliger et al., 1991) at their 3′ termini (designated by [3′T]). In subsequent experiments, we found that the single-stranded region at the 5′ end of ligand 20t is not important for high-affinity binding. Furthermore, the trinucleotide loops on helices II and III in ligand 36t (GCA and CCA) can be replaced with nonnucleotide (pentaethylene glycol) spacers (data not shown). These experiments provide further support for the importance of the helix junction region in high-affinity binding to PDGF-AB.

Binding Affinity of Minimal DNA Ligands to PDGF Isoforms. The binding of minimal ligands 20t, 36t, and 41t

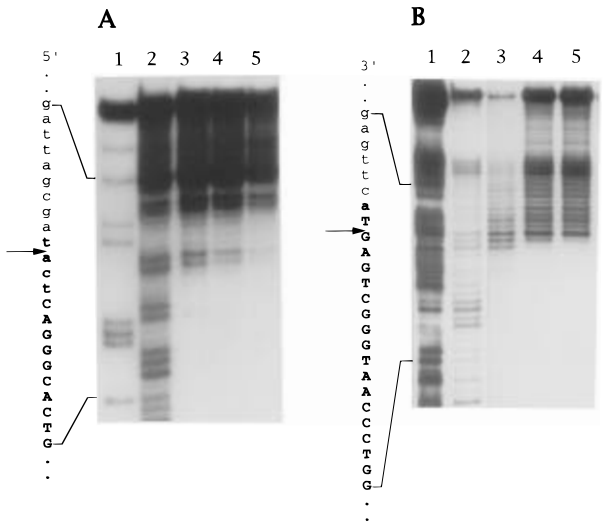

FIGURE 3: Determination of the minimal sequence requirement for a representative high-affinity ligand (41) to PDGF-AB. For the 5′ boundary (panel A), ^{32}P 3′ end-labeled ligand fragments serially truncated at the 5′ end by lambda exonuclease (lane 2) were incubated with 20 (lane 3), 5 (lane 4), and 0.5 (lane 4) nM PDGF-AB in binding buffer at 37 °C for 15 min followed by separation of the free from the PDGF-bound species by nitrocellulose filtration. The ligand fragments recovered from the filters were resolved on 8% polyacrylamide/7 M urea gels and visualized by autoradiography. Lane 1 is the ^{32}P 3′ end-labeled ligand partially modified with dimethyl sulfate and specifically cleaved 3′ to G bases (Maxam & Gilbert, 1980). For the 3′ boundary (panel B), the experiment was done with ^{32}P 5′ end-labeled ligand fragments serially truncated at the 3′ end by primer extension with deoxy- and dideoxynucleotides (same lane assignments as panel A, except lane 1 is a ddG sequencing marker lane). Arrows indicate the 5′ and 3′ boundaries suggested by the experiment. The boldface font shows the 5′ and 3′ ends of the truncated ligand 41 that was actually synthesized (adding two additional base pairs in stem 1 predicted from the model of the secondary structure in Figure 1). Lowercase and uppercase letters indicate nucleotides in the constant and evolved sequence regions, respectively.

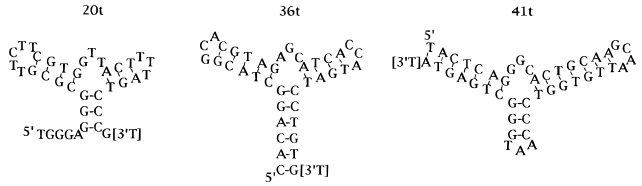

FIGURE 4: Folding of minimal DNA ligands 20t, 36t, and 41t according to the consensus secondary structure motif. [3′T] represents a 3′-3′-linked thymidine nucleotide added to reduce 3′-exonuclease-mediated degradation (Seliger et al., 1991).

to varying concentrations of PDGF-AA, PDGF-AB, and PDGF-BB in PBSM buffer at 37 °C is shown in Figure 5. In agreement with the binding properties of their full-length analogs, the minimal ligands bind to PDGF-AB and PDGF-BB with substantially higher affinity than to PDGF-AA. In fact, their affinity for PDGF-AA is comparable to that of random DNA. The binding to PDGF-AA is adequately described with a monophasic binding equation while the binding to PDGF-AB and PDGF-BB is notably biphasic. In previous SELEX experiments, we have found biphasic binding to be a consequence of the existence of separable nucleic acid species that bind to their target protein with different affinities (Jellinek et al., 1995; L.S.G. and N.J., unpublished results). The identity of the high- and low-affinity fractions is at present not known. Since the DNA ligands described here were synthesized chemically, it is

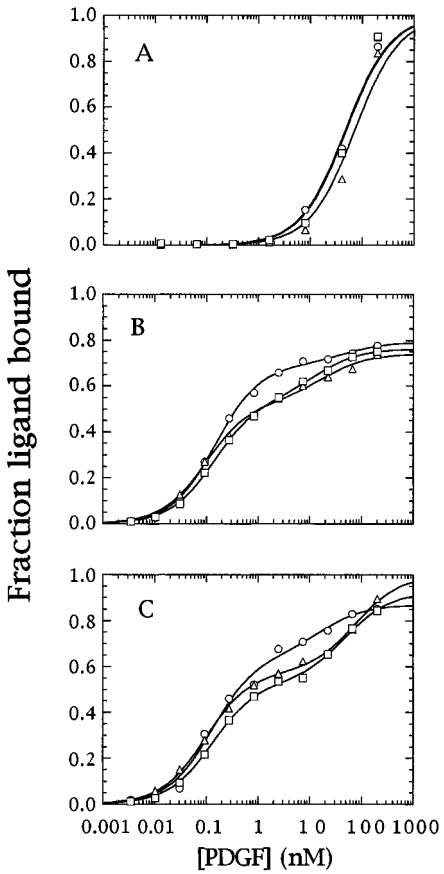

FIGURE 5: Binding of minimal DNA ligands to PDGF. The fraction of ^{32}P 5′ end-labeled DNA ligands bound to varying concentrations of PDGF-AA (panel A), PDGF-AB (panel B), and PDGF-BB (panel C) was determined by the nitrocellulose filter binding method. Minimal ligands tested were 20t (○), 36t (△), and 41t (□). Oligonucleotide concentrations in these experiments were ≈10 pM (PDGF-AB and PDGF-BB) and ≈50 pM (PDGF-AA). Data points were fitted to eq 1 (for binding of the DNA ligands to PDGF-AA) or to eq 2 (for binding to PDGF-AB and PDGF-BB) using the nonlinear least-squares method. Binding reactions were done at 37 °C in binding buffer (PBSM with 0.01% HSA).

possible that the ligand fraction that binds to PDGF-AB and PDGF-BB with lower affinity represents chemically imperfect DNA. Alternatively, the high- and the low-affinity species may represent stable conformational isomers that bind to the PDGF B-chain with different affinities. In any event, the higher affinity binding component is the most populated ligand species in all cases (Figure 5). For comparison, a 39-mer DNA ligand that binds to human thrombin with a K_d of 0.5 nM (ligand T39: 5′-CAGTCCGTGGTAGGGC-AGGTTGGGGTGACTTCGTGGAA[3′T]) and has a predicted stem−loop structure (Tasset at al., unpublished results) binds to PDGF-AB with a K_d of 0.23 μM (data not shown).

We also examined the binding of DNA ligands 20t, 36t, and 41t to PDGF-AB in PBS buffer containing 1 mM EDTA (PBSE) and found it to be comparable to the binding in PBSM buffer. Magnesium ion is therefore not essential for high-affinity binding. Incubation of PDGF-AB in 10 mM dithiothreitol for 1 h, on the other hand, reduces the binding affinity of these ligands by over 2 orders of magnitude (data not shown).

Dissociation Rates of Complexes of Minimal DNA Ligands with PDGF-AB. To evaluate the kinetic stability of the PDGF-AB/DNA complexes, we determined the dissociation rates at 37 °C for the complexes of minimal ligands 20t,

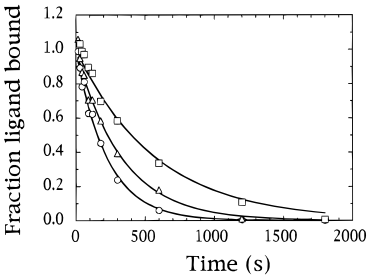

FIGURE 6: Dissociation rate determination for the high-affinity interaction between minimal DNA ligands and PDGF-AB. The fraction of 5′-^{32}P end-labeled ligands 20t (○), 36t (△), and 41t (□), all at 0.17 nM, bound to PDGF-AB (1 nM) was measured by nitrocellulose filter binding at the indicated time points following the addition of a 500-fold excess of the unlabeled competitor. The dissociation rate constant (k_{off}) values were determined by fitting the data points to eq 3. The experiments were performed at 37 °C in binding buffer.

36t, and 41t with PDGF-AB by measuring the amount of radiolabeled ligands (0.17 nM) bound to PDGF-AB (1 nM) as a function of time following the addition of a large excess of unlabeled ligands (Figure 6). At these protein and DNA ligand concentrations, only the high-affinity fraction of the DNA ligands binds to PDGF-AB. The following values for the dissociation rate constants were obtained by fitting the data points shown in Figure 6 to the first-order rate equation: $(4.5 \pm 0.2) \times 10^{-3}$ s^{-1} ($t_{1/2} = 2.6$ min) for ligand 20t, $(3.0 \pm 0.2) \times 10^{-3}$ s^{-1} ($t_{1/2} = 3.8$ min) for ligand 36t, and $(1.7 \pm 0.1) \times 10^{-3}$ s^{-1} ($t_{1/2} = 6.7$ min) for ligand 41t. The association rates calculated from the dissociation constants and dissociation rate constants ($k_{on} = k_{off}/K_d$) were $(3.1 \pm 0.3) \times 10^7$ M^{-1} s^{-1} for 20t, $(3.1 \pm 0.4) \times 10^7$ M^{-1} s^{-1} for 36t, and $(1.2 \pm 0.1) \times 10^7$ M^{-1} s^{-1} for 41t.

Thermal Melting Properties of Minimal DNA Ligands. To examine the ability of minimal ligands 20t, 36t, and 41t to assume folded structures, we determined their melting temperatures (T_m's) from the UV absorbance vs temperature profiles in PBSM or PBSE buffers (Figure 7). At the oligonucleotide concentrations used in these experiments (320−440 nM), only the monomeric species were observed as single bands on nondenaturing polyacrylamide gels (data not shown). Ligands 20t and 41t underwent thermal melting that is well described by a two-state (folded and unfolded) model with linearly sloping base lines (Petersheim & Turner, 1983) with T_m values in PBSM buffer of 43.8 ± 0.4 and 49.2 ± 0.5 °C, respectively. In PBSE buffer, similar T_m values were obtained: 44.8 ± 0.5 °C for ligand 20t and 48.0 ± 0.5 °C for ligand 41t (Figure 7A,C). Ligand 36t exhibited a more complex thermal melting profile in which two distinct transitions were observed (Figure 7B). In this case, the data were well described by a three-state model in which the fully folded and the unfolded states are connected through a partially unfolded intermediate (Dominic Zichi, unpublished results). Using this model, we obtained two T_m values for ligand 36t: 47.0 ± 0.9 and 67.1 ± 3.8 °C in PBSM buffer and 44.2 ± 1.7 and 64.3 ± 4.1 °C in PBSE buffer.

Photo-Cross-Linking of 5-Iodo-2′-deoxyuridine-Substituted Minimal DNA Ligands to PDGF-AB. To determine the sites on the DNA ligands and PDGF that are in close contact, we performed a series of photo-cross-linking experiments with 5-iodo-2′-deoxyuridine (IdU)-substituted DNA ligands 20t, 36t, and 41t. Upon monochromatic excitation at 308 nm, 5-iodo- and 5-bromo-substituted pyrimidine nucleotides

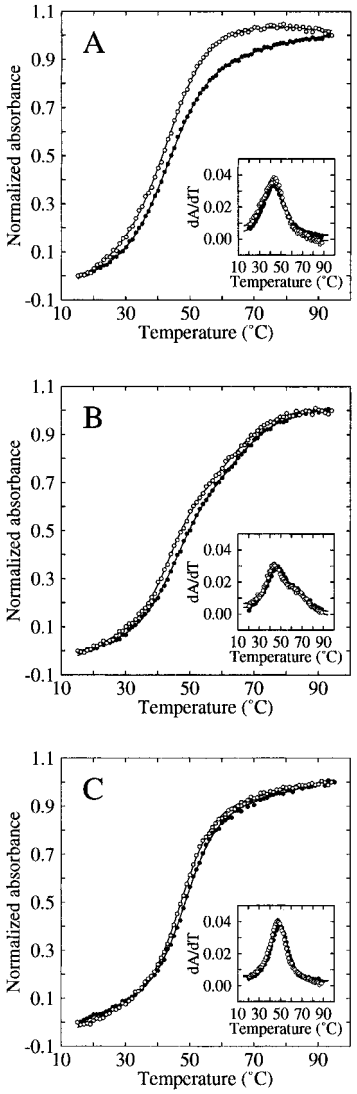

FIGURE 7: Thermal denaturation profiles for minimal DNA ligands to PDGF-AB. The absorbance change at 260 nm was measured in PBSM (○) or PBSE (●) as a function of temperature for ligands 20t (panel A), 36t (panel B), and 41t (panel C). Every 10th data point is shown for clarity. Data points were fitted according to a two-state thermal denaturation model for ligands 20t and 41t and to a three-state model for ligand 36t. First-derivative plots are shown in the insets.

populate a reactive triplet state following intersystem crossing from the initial n to π^* transition. The excited triplet state species then reacts with electron-rich amino acid residues (such as Trp, Tyr, His, and Phe) that are in its close proximity to yield a covalent cross-link. This method has been used extensively in studies of nucleic acid−protein interactions since it allows irradiation with >300 nm light which minimizes photodamage (Willis et al., 1993, 1994; Jensen et al., 1995; Stump & Hall, 1995). We synthesized analogs of ligands 20t, 36t, and 41t in which all thymidine residues were replaced with IdU residues using the solid phase phosphoramidite method. The affinity of these IdU-substituted ligands for PDGF-AB was somewhat enhanced compared to the unsubstituted ligands, and based on the appearance of bands with slower electrophoretic mobility on 8% polyacrylamide/7 M urea gels, all three 5′ end-labeled IdU-substituted ligands cross-linked to PDGF-AB upon irradiation at 308 nm (data not shown). The highest cross-linking efficiency was observed with IdU-substituted ligand

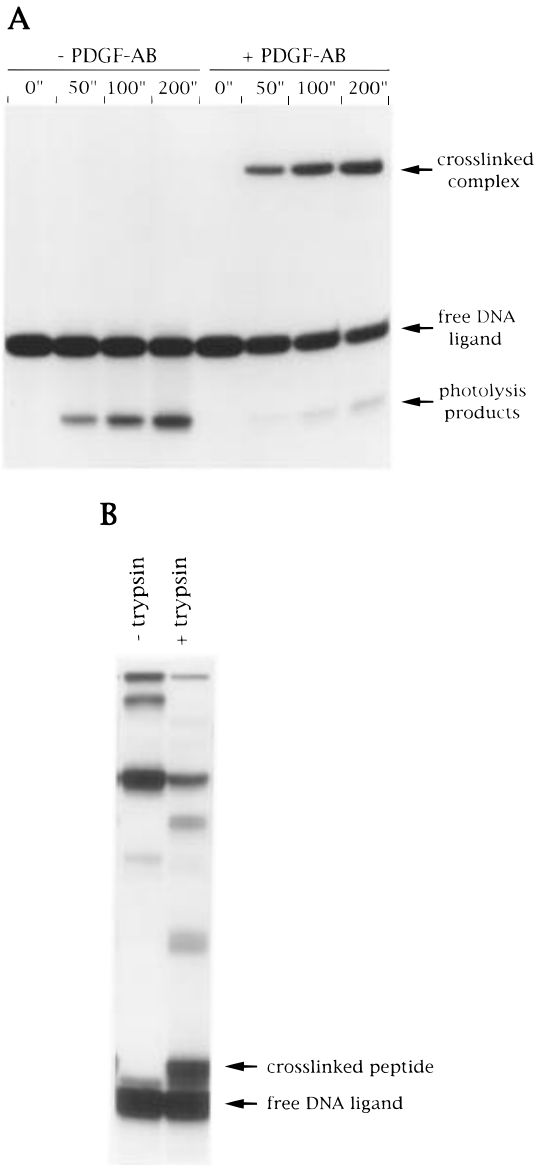

FIGURE 8: Photo-cross-linking of ligand 20t-I4 to PDGF-AB. In panel A, the autoradiogram of an 8% polyacrylamide/7 M urea gel indicates the appearance of cross-linked complex as a function of irradiation time in the presence, but not in the absence, of PDGF-AB. In panel B, the autoradiogram of an 8% polyacrylamide/7 M urea gel shows trypsin digestion of the cross-linked PDGF-AB/DNA complex. In the left-hand lane (undigested irradiated complex), the presence of mercaptoethanol (5% v/v) in the loading solution reveals multiple cross-linked species (compare with panel A). Free DNA (molecular mass = 12 kDa) and cross-linked tryptic peptide/ligand species used for amino acid sequencing are indicated.

20t. To identify the specific IdU position(s) responsible for the observed cross-linking, we tested seven singly or multiply IdU-substituted analogs of 20t for their ability to photo-cross-link to PDGF-AB: ligands 20t-I1 through 20t-I7 (5′-TGGGAGGGCGCGT^{1}T^{1}CT^{1}T^{1}CGT^{2}GGT^{3}T^{4}ACT^{5}T^{6}T^{6}T^{6}-AGT^{7}CCCG-3′ where the numbers indicate IdU substitutions at the indicated thymidine nucleotides for the seven ligands). Of these seven ligands, efficient cross-linking to PDGF-AB was observed only with ligand 20t-I4 (Figure 8A). The photo-reactive IdU position corresponds to the 3′ proximal thymidine nucleotide in the loop at the helix junction (Figure 4).

To identify the cross-linked amino acid residue(s) on PDGF-AB, a mixture of 5′ end-labeled 20t-I4 and PDGF-AB was incubated for 15 min at 37 °C followed by irradiation at 308 nm. The reaction mixture was then digested with modified trypsin, and the cross-linked fragments were resolved on an 8% polyacrylamide/7 M urea gel (Figure 8B). Edman degradation of the peptide fragment recovered from the band that migrated closest to the free DNA band revealed the amino acid sequence KKPIXKK, where X indicates a modified amino acid that could not be identified with the 20 derivatized amino acid standards. This peptide sequence, where X is phenylalanine, corresponds to amino acids 80−86 in the PDGF-B chain (Johnsson et al., 1984) (Figure 9A), which in the crystal structure of PDGF-BB comprises a part of solvent-exposed loop III (Oefner et al., 1992) (Figure 9B). In the PDGF A-chain, this peptide sequence does not occur (Betsholtz et al., 1986). Together, these data establish a point contact between a specific thymidine residue in ligand 20t and phenylalanine 84 of the PDGF B-chain.

Effect of Minimal DNA Ligands on PDGF-AA and PDGF-BB Binding to PDGF α- *and* β*-Receptors.* In order to determine whether the DNA ligands to PDGF were able to inhibit the effects of PDGF isoforms on cultured cells, we first determined their effects on binding of ^{125}I-labeled PDGF isoforms to PDGF α- and β-receptors stably expressed in porcine aortic endothelial (PAE) cells by transfection. Ligands 20t, 36t, and 41t all efficiently inhibited the binding of ^{125}I-PDGF-BB to PDGF α-receptors (Figure 10A) or PDGF β-receptors (data not shown), with half-maximal effects around 1 nM of DNA ligand. DNA ligand T39, directed against thrombin and included as a control, showed no effect. None of the ligands were able to inhibit the binding of ^{125}I-PDGF-AA to the PDGF α-receptor (Figure 10B), consistent with the observed specificity of ligands 20t, 36t, and 41t for PDGF-BB and PDGF-AB.

Effect of Minimal DNA Ligands on the Mitogenic Effects of PDGF-BB. We furthermore investigated the ability of the DNA ligands to inhibit the mitogenic effects of PDGF-BB on PAE cells expressing PDGF β-receptors. As shown in Figure 11A, the stimulatory effect of PDGF-BB on [^{3}H]-thymidine incorporation was neutralized by ligands 20t, 36t, and 41t. Ligand 36t exhibited half-maximal inhibition at a concentration of 2.5 nM; ligand 41t was slightly more efficient and 20t slightly less efficient. The control ligand T39 had no effect. Moreover, none of the ligands inhibited the stimulatory effects of fetal calf serum on [^{3}H]thymidine incorporation in these cells (Figure 11B), showing that the inhibitory effects are specific for PDGF.

DISCUSSION

The SELEX process is a versatile method for identifying nucleic acids that bind to a variety of molecular entities with high affinity and specificity. The aim of the SELEX experiment described here was to identify DNA antagonists to PDGF, in view of the importance of PDGF in several proliferative disease states. The decision to use the PDGF-AB heterodimer for affinity selection was based on the expectation that some of the ligands in the affinity-enriched pool would preferentially bind to the A-chain, some to the B-chain, and some to the interface between the two chains. In a sense, our intent was to perform three SELEX experiments in one. Surprisingly, the specificity of all ligands tested was found to be for the PDGF B-chain, although the

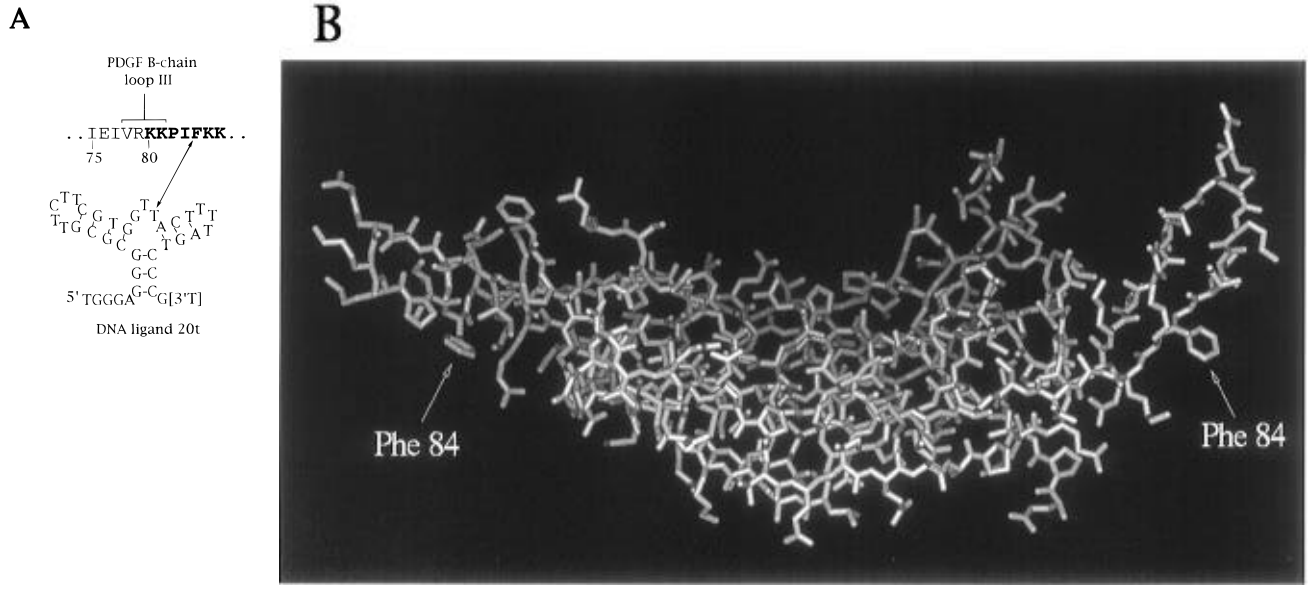

FIGURE 9: Point contact between DNA ligand 20t and PDGF B-chain identified by photo-cross-linking experiments. Panel A: Cross-linked tryptic peptide is shown in boldface letters, and the arrow denotes the point contact between a specific thymidine nucleotide and phenylalanine 84. Panel B: Crystal structure of the PDGF-BB homodimer according to Oefner at al. (1992) showing the solvent-exposed phenylalanine 84 residues. The distance between these phenylalanine residues in the crystal structure is ≈64 Å. For size comparison, a seven base pair DNA helix (assuming, for example, stacking of helices I and II in ligand 20t) is ≈21 Å in length.

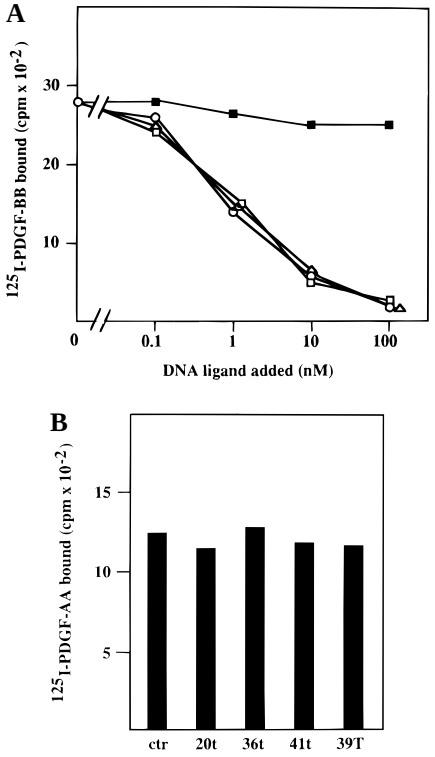

FIGURE 10: Effect of DNA ligands on PDGF-AA and PDGF-BB binding to PDGF α-receptors. Panel A: PAE cells expressing the PDGF α-receptor were incubated with 0.3 nM ^{125}I-PDGF-BB together with various concentrations of DNA ligands 20t (○), 36t (△), 41t (□), and T39 (■). Panel B: The same cells were incubated with 0.3 nM ^{125}I-PDGF-AA in the absence or presence of 100 nM DNA ligands. Unlabeled PDGF at 100 ng/mL reduced the binding of ^{125}I-PDGF-BB and PDGF-AA to 12 000 cpm and 2000 cpm, respectively.

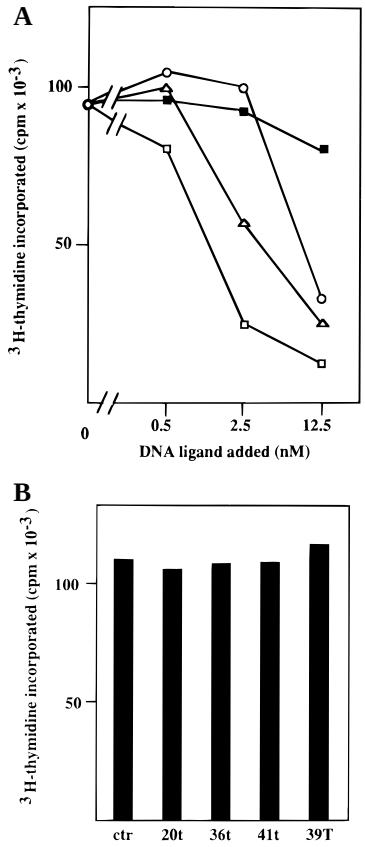

FIGURE 11: Effect of DNA ligands on PDGF-BB and fetal calf serum-induced [^{3}H]thymidine incorporation. Panel A: Serum-starved PAE cells expressing the PDGF β-receptor were incubated with 0.6 nM PDGF-BB together with [^{3}H]thymidine in the presence of various concentrations of DNA ligands 20t (○), 36t (△), 41t (□), and T39 (■). Panel B: The same cells were incubated with 10% fetal calf serum in the absence or presence of 12.5 nM DNA ligands. [^{3}H]Thymidine incorporation in the absence of PDGF or fetal calf serum was 16 000 cpm.

A- and the B-chains are ≈60% identical (Johnsson et al., 1984; Betsholtz et al., 1986). It is possible that we have not screened a sufficiently large population of ligands from the affinity-enriched pool to come across those ligands that preferentially bind to PDGF A-chain, or to the PDGF-AB heterodimer interface. Nevertheless, at equimolar concentrations (i.e., in the heterodimer), the PDGF B-chain appears

to have a greater propensity for binding to nucleic acids with high affinity compared to the A-chain. The fact that the B-chain is more basic than the A-chain may be a contributing factor. The development of high-affinity nucleic acid ligands to the PDGF A-chain will require the use of PDGF-AA in affinity selections. The selection for PDGF-AA ligands from the affinity-enriched library to PDGF-AB described here, in which the ligands that recognize the PDGF A-chain are at best sparse, represents an interesting alternative to selection from a new randomized library.

Inspection of the evolved sequences for the group of ligands shown in Figure 1 reveals short segments of primary structure conservation disrupted by less conserved sequence regions of variable length. In addition, the conserved regions are circularly permuted in several ligands (clones 2, 23, and 34 in group A and 31 and 41 in group B). The currently available multiple sequence alignment programs (as well as the human eye) are not very efficient in detecting such primary structure similarities. Alignment algorithms designed to look for shorter segments of sequence conservation, currently under development (Dominic Zichi and Brenda Javornik, unpublished results), may prove to be considerably more useful. The lack of a conserved contiguous sequence stretch of appreciable length makes the appropriate alignment difficult which in turn compounds the difficulty of identifying the consensus secondary structure. Indeed, the three-way helix junction motif was only noted upon inspection of energetically suboptimal folding structures for several ligands. Once this motif was identified, most of the ligands from the affinity-enriched pool were found to be capable of adopting it. A working secondary structure model allowed us to realign the sequences accordingly and subsequently detect the occurrence of significant base-pairing covariation in all three helices (Table 1), which, along with the minimal sequence information, provided further support for the model. To our knowledge, this is the first example of a three-way helix junction motif derived from a SELEX experiment.

Helix junctions are important elements of nucleic acid structure. A prominent and well-studied example is the four-way DNA junction, or Holliday junction, that plays an important role as a transiently occurring species in genetic recombination (Holliday, 1964; Seeman & Kallenbach, 1994). Three-way helix junctions are found in many RNA molecules including ribosomal RNA (Noller, 1984), the hammerhead ribozymes (Forster & Symons, 1987; Uhlenbeck, 1987), and snU4/U6 RNA (Guthrie & Patterson, 1988). DNA three-way junctions have been observed in electron micrographs (Minagawa et al., 1983) and are also believed to be important in recombinations events. Many proteins that bind to four-way DNA junctions also bind to three-way helix junctions (Jensch & Kemper, 1986; Duckett et al., 1992). As the simplest of the branched DNA structures, three-way junctions have been the subject of several recent structural and thermodynamic studies. These studies have shown that both the unpaired nucleotides at the branch point and divalent metal ions stabilize the structure of three-way DNA junctions by facilitating the coaxial stacking between two of the helices (Leonitis et al., 1991; Rosen & Patel, 1993a,b; Welch et al., 1993). The disposition of the helical arms with respect to one another is affected by divalent metal ions, by the number and composition of the single-stranded nucleotides at the branch point, and by the identity of base-paired nucleotides at the branch point (Rosen & Patel, 1993a,b; Welch et al., 1993, 1995; Seeman & Kallenbach, 1994; Zhong et al., 1994). For the high-affinity DNA ligands to the PDGF B-chain described here, strongly conserved nucleotides are found at the branch point where the number of unpaired nucleotides (three) is invariant (Figure 2). Surprisingly, magnesium ion does not appear to be required for either structure formation or binding to PDGF since the thermal melting and binding properties of minimal DNA ligands are similar in PBSM and PBSE buffers.

Table 2: Affinities of the Minimal DNA Ligands to PDGF-AA, PDGF-AB, and PDGF-BB

	K_d (nM)		
ligand	PDGF-AA[a]	PDGF-AB[b]	PDGF-BB[b]
20t	47 ± 4	0.147 ± 0.011	0.127 ± 0.031
36t	72 ± 12	0.094 ± 0.011	0.093 ± 0.009
41t	49 ± 8	0.138 ± 0.009	0.129 ± 0.011

[a] Data points shown in Figure 5A were fitted to eq 1 (Materials and Methods). [b] Data points in Figure 5B,C were fitted to eq 2. The dissociation constant (K_d) values shown represent the higher affinity binding component. The mole fraction of DNA that binds to PDGF-AB or PDGF-BB as the high-affinity component ranges between 0.58 and 0.88. The K_d values for the lower affinity interaction range between 13 to 78 nM.

Photo-cross-linking experiments have allowed us to establish a point contact between a specific thymidine residue in the helix junction loop region of ligand 20t and the PDGF B-chain phenylalanine 84. The region of the DNA ligands where conservation of primary and secondary structure elements is observed is thus in close proximity to the protein. It should be noted that cross-linking of the photoreactive DNA ligand to the PDGF B-chain occurs in the presence of the A-chain, since PDGF-AB was used in these experiments. This is consistent with the observed binding and inhibitory specificity of these ligands and indicates that cross-linking occurs at the functionally-relevant binding site.

According to the crystal structure model, PDGF-BB has an elongated shape in which each of the two disulfide-linked polypeptide chains consists of two antiparallel β-strands connected by three solvent-accessible loops. The two polypeptide chains are arranged in an antiparallel manner, placing all three loops on each end of the 2-fold symmetrical dimer (Oefner et al., 1992). Epitope mapping and mutagenesis studies have indicated that the amino acid residues near or at the solvent-accessible loops are involved in receptor binding (Giese et al., 1990; Clements et al., 1991; Östman et al., 1991; LaRochelle et al., 1992; Maher et al., 1993). Consistent with this notion is our observation that the binding of DNA ligands to the PDGF B-chain occurs in close proximity of loop III (phenylalanine 84) and that this binding prevents the interaction of PDGF-BB with PDGF α- and β-receptors.

In addition to receptor binding inhibition, all three minimal DNA ligands were also potent antagonists of the mitogenic effect of PDGF-BB and, by inference, PDGF-AB. It is interesting to note that the inhibitory efficiency of ligands 20t, 36t, and 41t is correlated with the relative stability of complexes of these ligands with PDGF-AB (Figure 6): *i.e.*, ligand 41t, which has the slowest dissociation rate, is the most potent inhibitor, and ligand 20t, which has the fastest dissociation rate, is the least potent inhibitor. For comparison, the dissociation constants of ligands 20t and 41t are similar (Figure 5, Table 2). Since the dissociation rate

of PDGF from the PDGF receptors is known to be very slow (Raines et al., 1990), the ability of these and other high-affinity ligands to inhibit the functional activity of PDGF may be intimately related to their ability to prevent receptor occupancy in a sustained manner.

Clinically useful PDGF antagonists would be highly desirable since PDGF overactivity has been observed in several disorders (Raines et al., 1990). Of importance in the use of antagonists is not to interfere with an essential normal function of PDGF. One effect of PDGF that needs to be taken into consideration is its effect on platelet aggregation. Human platelets contain PDGF α-receptors through which PDGF released from the platelets exerts a feedback mechanism to control platelet aggregation (Vassbotn et al., 1994). Inhibition of all PDGF isoforms may thus be accompanied by an excessive platelet aggregation. The involvement of PDGF in arterial lesion formation, *e.g.*, during the restenosis process, is likely to be exerted primarily via PDGF β-receptors on smooth muscle cells. Compounds that inhibit PDGF-AB and PDGF-BB but not PDGF-AA, such as those described in the present study, might have the desired properties of a PDGF antagonist for use to prevent restenosis, since they would prevent activation of PDGF β-receptors while retaining a partial response via the α-receptors.

The stability of nucleic acids to nucleases is an important consideration in efforts to develop nucleic acid-based therapeutics. Recent experiments in our laboratories have shown that many, and in some cases most, of the nucleotides in SELEX-derived ligands can be substituted with modified nucleotides that resist nuclease digestion in a manner that preserves and often enhances the binding affinity and specificity (Green et al., 1995a,b). Considerably improved stability was also observed with selectively modified hammerhead ribozymes (Pieken et al., 1991; Beigelman et al., 1995). Preliminary experiments of this type with the DNA ligands reported here suggest that substitutions with 2′-*O*-methyl- and 2′-fluoro-2′-deoxynucleotides are tolerated at many positions and that such substitutions impart substantially increased nuclease resistance (L.S.G. and N.J., unpublished results). These DNA ligands therefore represent lead compounds for a novel class of high-affinity, specific antagonists of PDGF-AB and PDGF-BB.

ACKNOWLEDGMENT

We thank Jeffrey Walenta for synthesis of DNA ligands, Brian Collins and Michael Willis for help with the excimer laser, Bruce Feistner for T_m measurements, and David W. McCourt for amino acid sequencing. We also thank Gudrun Bäckström for skillful technical assistance. We are especially thankful to Dominic Zichi and Brenda Javornik for developing the curve-fitting programs and for many helpful discussions. Finally, we thank Barry Polisky and Larry Gold for critical reading of the manuscript.

REFERENCES

Bates, D. M., & Watts, D. G. (1988) *Nonlinear Regression Analysis and its Applications*, Wiley, New York.

Beckmann, P. M., Betsholtz, C., Heldin, C.-H., Westermark, B., Di Marco, E., Di Fiore, P. P., Robbins, K. C., & Aaronson, S. A. (1988) *Science 241*, 1346−1349.

Beigelman, L., McSwiggen, J. A., Draper, K. G., Gonzalez, C., Jensen, K., Kapreisky, A. M., Modak, A. S., Matulic-Adamic, J., DiRenzo, A. B., Haeberli, P., Sweedler, D., Tracz, D., Grimm, S., Wincott, F. E., Thackray, V. G., & Usman, N. (1995) *J. Biol. Chem. 270*, 25702−25708.

Betsholtz, C., Westermark, B., Ek, B., & Heldin, C.-H. (1984) *Cell 39*, 447−457.

Betsholtz, C., Johnsson, A., Heldin, C.-H., Westermark, B., Lind, P., Urdea, M. S., Eddy, R., Shows, T. B., Philpott, K., Mellor, A. L., Knott, T. J., & Scott, J. (1986) *Nature 320*, 695−699.

Boström, H., Willets, K., Pekny, M., Levéen, P., Lindahl, P., Hedstrand, H., Pekna, M., Hellström, M., Gebre-Medhin, S., Schalling, M., Nilsson, M., Kurland, S., Törnell, J., Heath, J. K., & Betsholtz, C. (1996) *Cell 85*, 863−873.

Buchdunger, E., Zimmerman, J., Mett, H., Meyer, T., Müller, M., Regenass, U., & Lydon, N. B. (1995) *Proc. Natl. Acad. Sci. U.S.A. 92*, 2558−2562.

Bywater, M., Rorsman, F., Bongcam-Rudloff, E., Mark, G., Hammacher, A., Heldin, C.-H., Westermark, B., & Betsholtz, C. (1988) *Mol. Cell. Biol. 8*, 2753−2762.

Claesson-Welsh, L. (1994) *J. Biol. Chem. 269*, 32023−32026.

Claesson-Welsh, L., Eriksson, A., Westermark, B., & Heldin, C.-H. (1989) *Proc. Natl. Acad. Sci. U.S.A. 86*, 4917−4921.

Clements, J. M., Bawden, L. J., Bloxidge, R. E., Catlin, G., Cook, A. L., Craig, S., Drummond, A. H., Edwards, R. M., Fallon, A., Green, D. R., Hellewell, P. G., Kirwin, P. M., Nayee, P. D., Richardson, S. J., Brown, D., Chahwala, S. B., Snarey, M., & Winslow, D. (1991) *EMBO J. 10*, 4113−4120.

Doolittle, R. F., Hunkapiller, M. W., Hood, L. E., Devare, S. G., Robbins, K. C., Aaronson, S. A., & Antoniades, H. N. (1983) *Science 221*, 275−277.

Duan, D.-S. R., Pazin, M. J., Fretto, L. J., & Williams, L. T. (1991) *J. Biol. Chem. 266*, 413−418.

Duckett, D. R., Murchie, A. I. H., Bhattacharyya, R. M., Clegg, R. M., Diekmann, S., von Kitzing, E., & Lilley, D. M. J. (1992) *Eur. J. Biochem. 207*, 285−295.

Eaton, B. E., Gold, L., & Zichi, D. A. (1995) *Chem. Biol. 2*, 633−638.

Ellington, A., & Szostak, J. (1990) *Nature 346*, 818−822.

Engström, U., Engström, Å., Ernlund, A., Westermark, B., & Heldin, C.-H. (1992) *J. Biol. Chem. 267*, 16581−16587.

Ferns, G. A. A., Raines, E. W., Sprugel, K. H., Motani, A. S., Reidy, M. A., & Ross, R. (1991) *Science 153*, 1129−1132.

Forster, A. C., & Symons, R. H. (1987) *Cell 49*, 211−220.

Giese, N., LaRochelle, W. J., May-Siroff, M., Robbins, K. C., & Aaronson, S. A. (1990) *Mol. Cell. Biol. 10*, 5496−5501.

Gill, S. C., & von Hippel, P. H. (1989) *Anal. Biochem. 182*, 319−326.

Gold, L. (1995) *J. Biol. Chem. 270*, 13581−13584.

Gold, L., Polisky, B., Uhlenbeck, O. C., & Yarus, M. (1995) *Annu. Rev. Biochem. 64*, 763−797.

Green, L. S., Jellinek, D., Bell, C., Beebe, L. A., Feistner, B. D., Gill, S. C., Jucker, F. M., & Janjic, N. (1995a) *Chem. Biol. 2*, 683−695.

Green, L., Waugh, S., Binkley, J. P., Hostomska, Z., Hostomsky, Z., & Tuerk, C. (1995b) *J. Mol. Biol. 247*, 60−68.

Guthrie, C., & Patterson, B. (1988) *Annu. Rev. Genet. 22*, 387−419.

Heldin, C.-H. (1992) *EMBO J. 11*, 4251−4259.

Heldin, C.-H., Bäckström, G., Östman, A., Hammacher, A., Rönnstrand, L., Rubin, K., Nistér, M., & Westermark, B. (1988) *EMBO J. 7*, 1387−1394.

Heldin, C.-H., Ernlund, A., Rorsman, C., & Rönnstrand, L. (1989) *J. Biol. Chem. 264*, 8905−8912.

Herren, B., Weyer, K. A., Rouge, M., Lötscher, P., & Pech, M. (1993) *Biochim. Biophys. Acta 1173*, 294−302.

Holliday, R. (1964) *Genet. Res. 5*, 282−304.

Iida, H., Seifert, R., Alpers, C. E., Gronwald, R. G. K., Phillips, P. E., Pritzl, P., Gordon, K., Gown, A. M., Ross, R., Bowen-Pope, D. F., & Johnson, R. J. (1991) *Proc. Natl. Acad. Sci. U.S.A. 88*, 6560−6564.

Irvine, D., Tuerk, C., & Gold, L. (1991) *J. Mol. Biol. 222*, 739−761.

Jellinek, D., Lynott, C. K., Rifkin, D. B., & Janjic, N. (1993) *Proc. Natl. Acad. Sci. U.S.A. 90*, 11227−11231.

Jellinek, D., Green, L. S., Bell, C., & Janjic, N. (1994) *Biochemistry 33*, 10450−10456.

Jellinek, D., Green, L. S., Bell, C., Lynott, C. K., Gill, N., Vargeese, C., Kirschenheuter, G., McGee, D. P. C., Abesinghe, P., Pieken, W. A., Shapiro, R., Rifkin, D. B., Moscatelli, D., & Janjic, N. (1995) *Biochemistry 34*, 11363−11372.
Jensch, F., & Kemper, B. (1986) *EMBO J. 5*, 181−189.
Jensen, K. B., Atkinson, B. L., Willis, M. C., Koch, T. H., & Gold, L. (1995) *Proc. Natl. Acad. Sci. U.S.A. 92*, 12220−12224.
Johnsson, A., Heldin, C.-H., Wasteson, A., Westermark, B., Deuel, T. F., Huang, J. S., Seeburg, P. H., Gray, A., Ullrich, A., Scrace, G., Stroobant, P., & Waterfield, M. D. (1984) *EMBO J. 3*, 921−928.
Johnsson, A., Betsholtz, C., Heldin, C.-H., & Westermark, B. (1985) *Nature 317*, 438−440.
Kovalenko, M., Gazit, A., Böhmer, A., Rorsman, C., Rönnstrand, L., Heldin, C.-H., Waltenberger, J., Böhmer, F.-D., & Levitzki, A. (1994) *Cancer Res. 54*, 6106−6114.
LaRochelle, W. J., Robbins, K. C., & Aaronson, S. A. (1989) *Mol. Cell. Biol. 9*, 3538−3542.
LaRochelle, W. J., Pierce, J. H., May-Siroff, M., Giese, N., & Aaronson, S. A. (1992) *J. Biol. Chem. 267*, 17074−17077.
Leonitis, N. B., Kwok, W., & Newman, J. S. (1991) *Nucleic Acids Res. 19*, 759−766.
Levéen, P., Pekny, M., Gebre-Medhin, S., Swolin, B., Larsson, E., & Betsholtz, C. (1994) *Genes Dev. 8*, 1875−1887.
Lindner, V., & Reidy, M. A. (1995) *Am. J. Pathol. 146*, 1488−1497.
Lindner, V., Giachelli, C. M., Schwartz, S. M., & Reidy, M. A. (1995) *Circ. Res. 76*, 951−957.
Maher, D. W., Strawn, L. M., & Donoghue, D. J. (1993) *Oncogene 8*, 533−541.
Matsui, T., Heidaran, M., Miki, T., Popescu, N., La Rochelle, W., Kraus, M., Pierce, J., & Aaronson, S. A. (1988) *Science 243*, 800−804.
Maxam, A. M., & Gilbert, W. (1980) *Methods Enzymol. 65*, 499−559.
Minagawa, T., Murakami, A., Ryo, Y., & Yamagishi, H. (1983) *Virology 126*, 183−193.
Mori, S., Claesson-Welsh, L., & Heldin, C.-H. (1991) *J. Biol. Chem. 266*, 21158−21164.
Noller, H. F. (1984) *Annu. Rev. Biochem. 53*, 119−162.
Oefner, C., D'Arcy, A., Winkler, F. K., Eggiman, B., & Hosang, M. (1992) *EMBO J. 11*, 3921−3926.
Östman, A., Andersson, M., Hellman, U., & Heldin, C.-H. (1991) *J. Biol. Chem. 266*, 10073−10077.
Pagratis, N. (1996) *Nucleic Acids Res. 24*, 3645−3646.
Petersheim, M., & Turner, D. H. (1983) *Biochemistry 22*, 256−263.
Pieken, W. A., Olsen, D. B., Benseler, F., Aurup, H., & Eckstein, F. (1991) *Science 253*, 314−317.
Raines, E. W., Bowen-Pope, D. F., & Ross, R. (1990) in *Handbook in Experimental Pharmacology. Peptide Growth Factors and Their Receptors* (Sporn, M. B., & Roberts, A. B., Eds.) pp 173−262, Springer, Heidelberg.
Rosen, M., & Patel, D. J. (1993a) *Biochemistry 32*, 6563−6575.
Rosen, M., & Patel, D. J. (1993b) *Biochemistry 32*, 6576−6587.
Sambrook, J., Fritsch, E. F., & Maniatis, T. (1989) *Molecular Cloning: A Laboratory Manual*, 2nd ed., Cold Spring Harbor Laboratory Press, Cold Spring Harbor, NY.
Seeman, N. C., & Kallenbach, N. R. (1994) *Annu. Rev. Biophys. Biomol. Struct. 23*, 53−86.
Seifert, R. A., Hart, C. E., Phillips, P. E., Forstrom, J. W., Ross, R., Murray, M. J., & Bowen-Pope, D. F. (1989) *J. Biol. Chem. 264*, 8771−8778.
Seliger, H., Froehlich, A., Montenarh, A., Ramalho Ortigao, J. F., & Roesch, H. (1991) *Nucleosides Nucleotides 10*, 469−477.
Sinha, D. N., Biernat, J., McManus, J., & Koester, H. (1984) *Nucleic Acids Res. 12*, 4539−4557.
Soriano, P. (1994) *Genes Dev. 8*, 1888−1896.
Stump, W. T., & Hall, K. B. (1995) *RNA 1*, 55−63.
Teisman, J., & Hart, C. E. (1993) *J. Biol. Chem. 268*, 9621−9628.
Tuerk, C., & Gold, L. (1990) *Science 249*, 505−510.
Tuerk, C., Eddy, S., Parma, D., & Gold, L. (1990) *J. Mol. Biol. 213*, 749−761.
Uhlenbeck, O. C. (1987) *Nature 328*, 596−600.
Vassbotn, F. S., Langeland, N., Hagen, I., & Holmsen, H. (1990) *Biochim. Biophys. Acta 1054*, 246−249.
Vassbotn, F. S., Östman, A., Siegbahn, A., Holmsen, H., & Heldin, C.-H. (1992) *J. Biol. Chem. 267*, 15635−15641.
Vassbotn, F. S., Havnen, O. K., Heldin, C.-H., & Holmsen, H. (1994) *J. Biol. Chem. 269*, 13874−13879.
Waterfield, M. D., Scrace, G. T., Whittle, N., Stroobant, P., Johnsson, A., Wasteson, A., Westermark, B., Heldin, C.-H., Huang, J. S., & Deuel, T. F. (1983) *Nature 304*, 35−39.
Welch, J. B., Duckett, D. R., & Lilley, D. M. J. (1993) *Nucleic Acids Res. 21*, 4548−4555.
Welch, J. B., Walter, F., & Lilley, D. M. J. (1995) *J. Mol. Biol. 251*, 507−519.
Williams, L. T., Trimble, P. M., Lavin, M. F., & Sunday, M. E. (1984) *J. Biol. Chem. 259*, 5287−5294.
Willis, M. C., Hicke, B. J., Uhlenbeck, O. C., Cech, T. R., & Koch, T. H. (1993) *Science 262*, 1255−1257.
Willis, M. C., LeCuyer, K. A., Meisenheimer, K. M., Uhlenbeck, O. C., & Koch, T. H. (1994) *Nucleic Acids Res. 22*, 4947−4952.
Yarden, Y., Escobendo, J. A., Kuang, W.-J., Yang-Feng, T. L., Daniel, T. O., Tremble, P. M., Chen, E. Y., Ando, M. E., Harkins, R. N., Francke, U., Friend, V. A., Ullrich, A., & Williams, L. T. (1986) *Nature 323*, 226−232.
Zhong, M., Rashes, M. S., Leonitis, N. B., & Kallenbach, N. R. (1994) *Biochemistry 33*, 3660−3667.

BI961544+